CITY ALIEN

EREZ GATI

IGOR LABUTOV

CARLOS JARAMILLO

RICARDO CHINCHA

FERNANDO GUEVARA

Required Faculty Advisor Statement:

I certify that the engineering design of the vehicle described in this report, City Alien, has been significant and that each team member has earned four semester hours, of senior design credit for their work on this project.

Professor **Jizhong Xiao**
Department of Electrical Engineering, City College

1. Introduction

City ALIEN is a radically redesigned platform from the City College's 2009 entry - ELVIS. The new design is based on an achieved consensus of team members to strike a balance between *innovation* and *improvement*. The team did not want to merely improve performance of the last year's robot by fine-tuning existing platform; the team wanted to experiment with cutting-edge research in computer vision as means to dramatically enhance performance. From the experience of 2009 IGVC, the following issues were noted to be primary for the failure to complete Autonomous Competition (72% of course completed):

- **Lane detection false positives** In situations with bright obstacles (such as cones), false lane positives misguided the obstacle avoidance algorithm. This caused the eventual failure at the 72% mark.
- **Poor speed-control on ramps** Custom-designed speed control routine failed to "brake" the motors on downhill slopes, causing it to accelerate and loose control. Heavy rain did not help the situation.
- **Laser scanner failed to detect obstacles early** Laser scanner was mounted as to pitch above the horizon to avoid mistaking the ground (on downhill slopes) for obstacles. This, however, directly reduced the range at which low obstacles (such as cones) were detected.

In addition, the City College team will be participating in the Navigation and JAUS challenges for the first time, which required development from the ground-up. Next we discuss how the issues above are addressed, and the innovations which they inspired.

2. Innovations

Each of the above-mentioned failures was analyzed in detail upon arrival from the competition in 2009 (and re-enacted on a home test field to support the hypotheses). The following solutions were proposed:

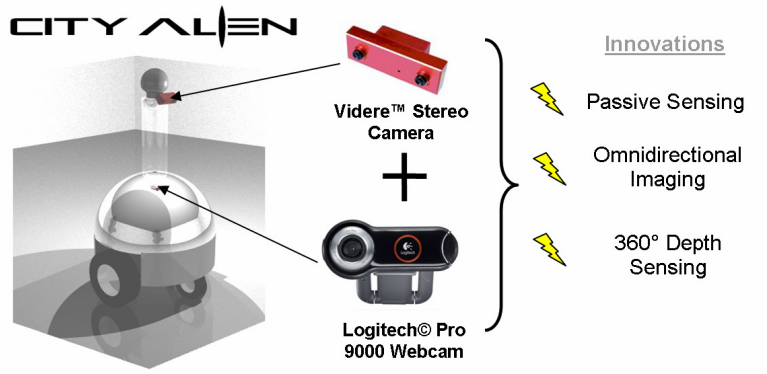

Figure 1 Sensing Innovation

- **Cutting-edge concept in vision-only sensing** The Omnidirectional Catadioptric (combination of mirrors and optics) Stereo is an intriguing concept introduced recently by G. Jang *et al** which calls for a single camera and a clever mirror and optics arrangement (*def.* catadioptrics) to provide depth cues in a 360° panorama. Essentially this alleviates the need for a laser scanner, making the vehicle completely **passive** and undetectable in surveillance applications. Most importantly, obstacle-sensing is no longer constrained to a plane, thus removing the problem of near-sightedness when the scanner is pitched.
- **Robust lane detection in presence of clutter** The primary reason for false-positive lanes is when bright and long obstacles (such as tall cones) are treated as lanes. We avoid this situation at its root, by detecting obstacles (through color and stereo) and masking them from the image prior to lane detection (in effect isolating lanes)
- **Dynamic Braking using H-Bridge** The main improvement to the electronics system from ELVIS, is the introduction of the dynamic brake mechanism in the H-Bridge itself. Because all electronics were designed from scratch, the team was intimately familiar with its operation, and the improvement was deemed possible. Dynamic braking essentially

* G. Jang, S. Kim, and I. Kweon, "Single camera catadioptric stereo system," Proc. of Workshop on Omnidirectional Vision, Camera Networks and Nonclassical cameras (OMNIVIS2005), 2005.

shorts the motor windings at high frequency, giving the illusion of a continuously-variable brake, without the complexity of an actual ABS system.

- **Waterproofing** Although heavy rain did not cause problems to ELVIS (besides slippage), it was a miracle that it didn't. This year, the team decided not to take chances, and instead exploit the unique geometry of the robot (the mirror dome) as a watertight container housing the electronics.

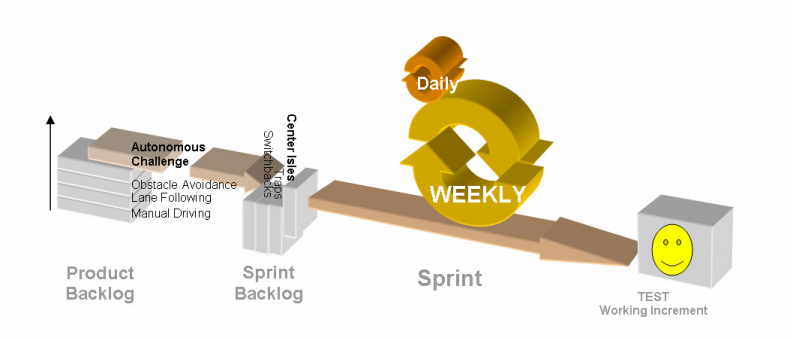

Figure 2 Agile development model

3. Agile Collaboration Model

The drastic technical innovations proposed above called for an innovation in planning methodology as well. The scope of innovation called for a multidisciplinary team and the tight time budget for a careful risk assessment (a risk of not completing the robot in time) at each stage of the development cycle. An **Agile** collaboration model has been researched and found appropriate for our use. The three pillars of Agile model include:

- **Self-organizing, evolving team** *over fixed labor division*. It is a nature of an undergraduate student to be verse (relatively) in many fields at once, because of the natural breadth of undergraduate schooling. It is therefore imprudent to fix a team member to one task, if his knowledge and skill can be tapped in several areas.
- **Quick iterations** *over exhaustive planning*. Concept→Design→Test→Redesign cycle allows for immediate evaluation of a new concept – such as our innovative vision system. Too much planning without immediate feedback would be foolish.

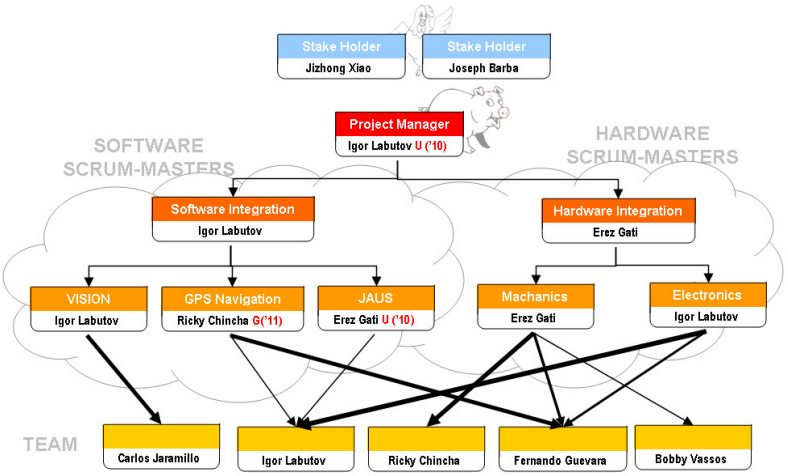

Figure 3 Agile team organization

- **Responding to change** *over following a plan (Risk assessment).* Does not imply that planning is unimportant. Instead, good planning must be malleable in situations where a design proves impractical. In our case - experimental vision research carried a significant amount of risk, thus a back-up laser scanner was maintained.

The functional unit of an Agile cycle is a SCRUM – a temporary team that produces a testable result over a period of 1-2 weeks. It begins with a "Product Backlog" – a priority queue, mandated by the product specifications – Competition rules in our case. A task, once popped from the "Product Backlog" queue is tackled by a self-organized team of 2 or 3 people that meet everyday (in a "sprint") and produce a testable product at the end of the cycle. Using this approach, we were able to

produce testable hardware and software in short bursts without the risk of over-planning and not meeting a deadline. In Figure 3, our team organization within the Agile paradigm is presented. SCRUM-masters are responsible for maintaining the "Sprint Backlog" (a kind of local task queue) and pacing the SCRUM.

4. Design Cycle

The overview of our design cycle is presented in Figure 4. The novel concept of an omnidirectional stereo rig was first conceptualized (Fig. 4.1) based on the latest research in computer vision and robotics. The concept had then gone through a CAD design stage (Fig 4.2) where, in addition to the unique optical geometry of the platform, electronics, actuators and wiring were placed such as to satisfy the rules of the competition. Based on the CAD model, a simulation of the optics and catadioptrics was performed using a ray-tracer (POVray). After feasibility of the idea was validated in simulation, a scale model was developed under real-world conditions. Finally, a life-size prototype was constructed to test the scalability of the system, only after which the final prototype was constructed. Typically, each step had involved modifications and returns to the drawing board. More specifically, the optics (size and separation of the mirrors) had to be tuned exactly to achieve the desired performance of the vision system. The details of these steps will be discussed next.

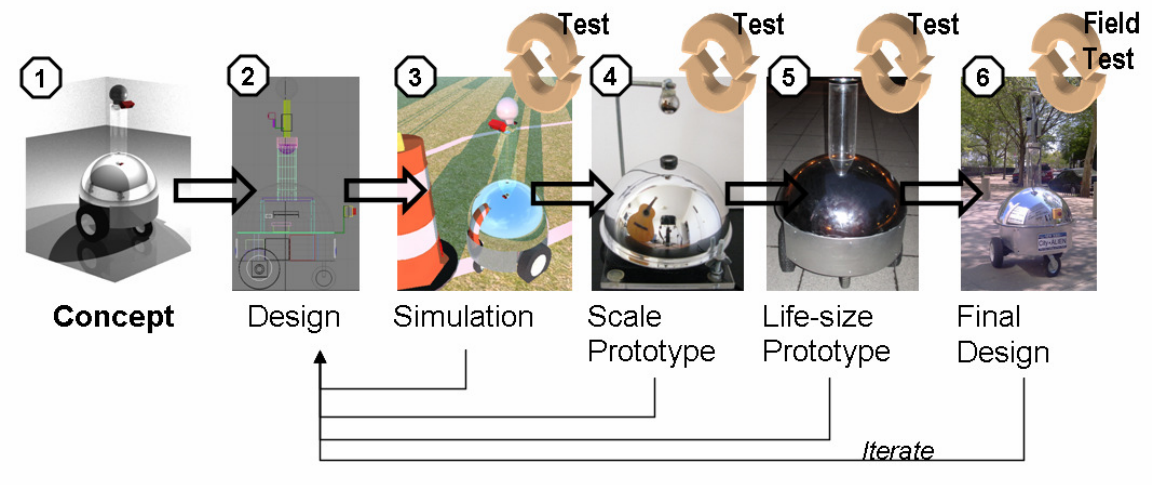

Figure 4 Design Cycle

We shall first discuss the central innovation of our design, before connecting it with the rest of the system, such as to give the reader the value of this novel concept in the context of the complete design.

5. Design of the Novel Omnidirectional Stereo Rig

The concept behind an omnidirectional stereo rig dates back to the research originally conducted by Nayar and his colleagues in Columbia University*. The idea is simple – instead of using two cameras to produce stereo geometry for triangulation, use one camera and two mirrors! If the mirrors have rotation symmetry and the camera is coaxially aligned with the mirrors, then not only do you get stereo, but 360° stereo! The idea behind our design, however, is novel and differs from the traditional omnidirectional stereo rig in several important aspects:

- **Spherical Mirrors** All research in such rigs utilize complex hyperbolic mirrors that are *costly* and difficult to manufacture. We use simple hemispheres. However, while a single sphere is easily usable for a one-mirror system,

* Shree K. Nayar, Venkata Peri, "Folded catadioptric cameras," CVPR2 pp.2217, 1999 IEEE Computer Society Conference on Computer Vision and Pattern Recognition (CVPR'99) - Volume 2, 1999.

using two spheres (for stereo) makes it difficult to obtain the desired field-of-view and resolution. We model the system and find the optimal relationship between mirrors' radii and separation.

- **"Catadioptric Enclosure"** Our camera is essentially the entire robot. One of its mirrors covers and protects (waterproof) electronics including the computer. The second mirror at the top of the plexiglass tube supports the wireless E-Stop antenna, compass and the GPS antenna. Larger mirrors provide better resilience to scratches and damage, and a large separation between the mirrors (baseline) offers the ability to "sense" depth much farther then would be possible with a small stereo unit (at the expense of resolution, of course)

5.1 Model

Figure 7 depicts the model of our design. Two mirrors coaxially aligned with a single camera pointing *up* (*F* in Fig. 7) are separated by distance *H* (71cm). The camera observes the *minor* mirror directly, and the *major* mirror through its reflection in the *minor* mirror. The final image looks like Fig. 5C – two concentric circular images. The triangulation works as follows: an image of a cone (Fig 5A) can be traced back through two rays (*a* to *minor* mirror and *A* to *major* mirror), which produces a double image of a cone. By tracing the rays back from the two images, we can calculate the distance to the cone. Note that the cone appears on the same radial line in both the outer and the inner images (Figure 6 illustrates the same concept but with the barrel. Fig 6C shows a panoramic unwrapping of the inner and outer images, where radial symmetric conveniently turns into vertical symmetry)

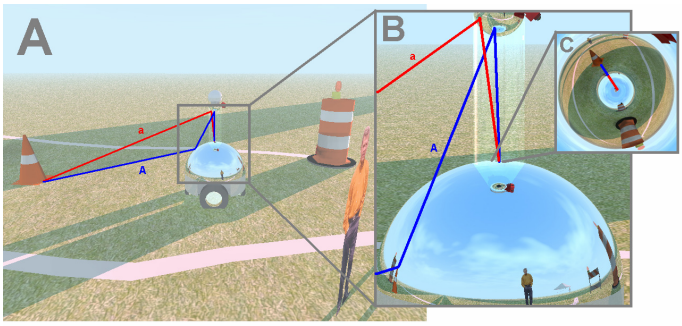

Figure 5 Concept of Catadioptric Stereo

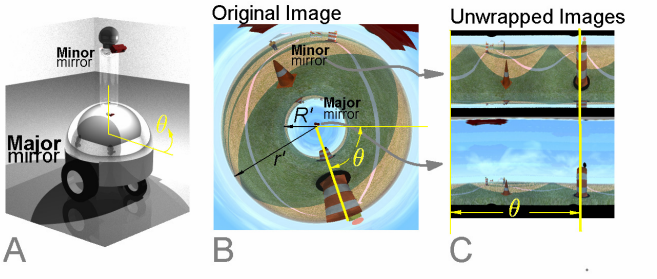

Figure 6 Catadioptric image-formation

5.2 Optimization

In our research with the spherical-mirror stereo concept, we have analyzed the effect of the relative size of the two mirrors and their separation on the produced image. Using a symbolic mathematical package (MuPad™), we derived the equations of the system which determine two properties of the system important to us – Vertical Field-of-view (FOV for short), and the relative sizes of the *imaged* mirrors R'/r' (Fig. 6B). A good ratio (1:2 – 1:4) essentially guarantees that both the inner and outer images will be of sufficient resolution to be of practical use. What we have discovered, is that the effect of the mirrors' radii is essentially linear (Fig. 8) with the Field of View and

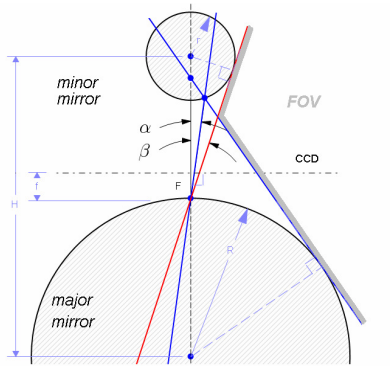

Figure 7 Geometric Model

the ratio. Moreover the two are inversely related. This allowed us to linearize the model into the two simple design equations, which we can then solve to yield optimal results.

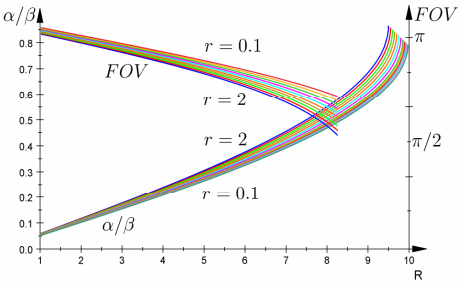

Figure 8 Model parameter space

$$\frac{r'}{R'} = \frac{R}{\sqrt{2}H} \quad (1)$$

$$FOV_v = \pi - \frac{R}{H} \quad (2)$$

Note, these equations, like all linearizations break down at some critical value (from the graph, it is clear that as the mirrors become comparable in size, the approximation deteriorates). In effect, we used them as more of a rule-of-thumb to get the approximate design parameters, and then fine-tune them in simulation.

5.3 Simulation

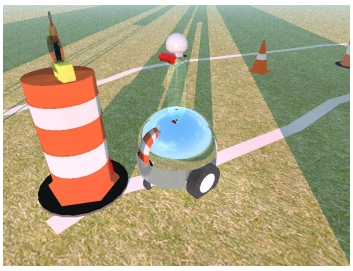

Figure 9 Ray-tracer simulation of IGVC field

Typically, with today's abundance of robotics' simulation tools, there is hardly a need to develop a custom one. However, no simulation on a market today is able to produce a physically accurate simulation of optics – a foremost requirement to validate our design. As such, the only viable computation tool for this task is a ray-tracer. Albeit slow, the ray-tracer allows one to simulate complex systems of mirrors and optics such as ours. POVray – a free and open-source ray tracer was used to generate synthetic imagery of an IGVC field and to select the optimum sizes of the *minor* and *major* mirrors. An optimal (field-of-view and resolution) rig was simulated with the following parameters:

TABLE I
DESIGN PARAMETERS FOR A SIMULATED SYSTEM

Parameter	*R*	*r*	*H*	r'/R'	*FOV*
Value (cm)	40cm	5cm	70	1/3	153°

Values satisfy the design constraints $H \geq 2R$ and $R \geq 2r$ for the model

5.4 Prototypes

A scale prototype (R=5.25cm) was constructed to test the feasibility of the sensor in the real world. The same camera was utilized in the scale model as in the final design (Logitech Pro-9000). The depth-images obtained with the scale prototype were on-par with the results from simulation and were promising enough to warrant the construction of a full-scale prototype. The performance on the static full-scale prototype gave the green light for the finalization of the design and the parameters (listed in Table 2)

TABLE 2
DESIGN PARAMETERS FOR THE REAL-WORLD PROTOTYPES

Parameter:	*R*	*r*	*H*	α / β	*FOV*
Scale	5.25cm	0.7cm	10.5cm	0.35 ≈ 1/3	151°
Life-size	40.6cm	5.25cm	71.1cm	0.40 = 2/5	147.3°

Values satisfy the design constraints $H > R >> r$ for the model

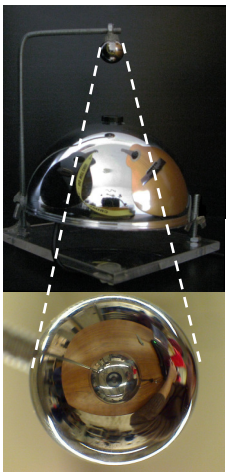

Figure 9 Scale prototype

6 Sensing Strategy

Although vision is the ALIEN's sole sense of the world, it has more than one eye and a pair of mirrors. A second, conventional stereo head is used to complement the omnidirectional stereo system described above. The decision to fuse two cameras was motivated by their unique strengths and weaknesses. While the omnidirectional-stereo system provides an ultra-wide field-of-view, it has a fairly poor resolution (as two 360° images have to fit into one 320x240 frame). The B/W Videre Design© STOC (Stereo-on-chip) camera is utilized to provide high-resolution frontal depth-imaging of the field, where resolution is critical.

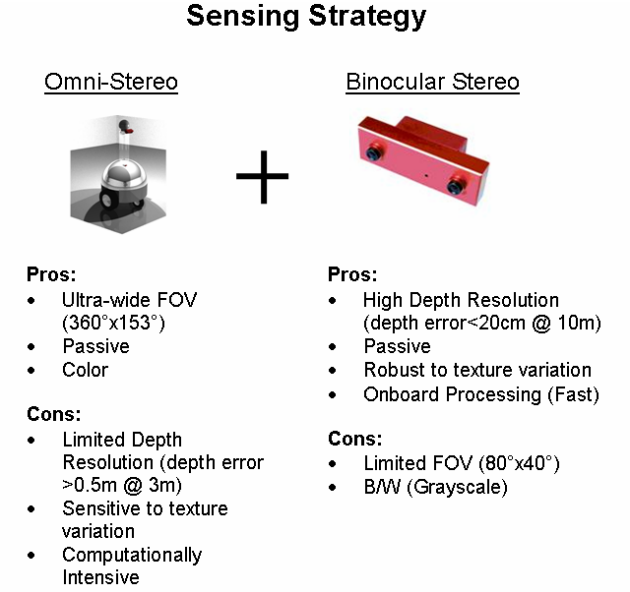

6.1 Camera Fusion

The information from both cameras are fused into a central occupancy grid that is used for path planning (described in Section 8). Omnidirection stereo system, by the virtue of its radial symmetricity, is most conveniently mapped into a polar occupancy grid (r, θ), while the narrow field-of-view binocular sterem camera is mapped into cartesian occupancy grid (x,y). The process of generating the respective occupancy grids is is summarized in two subsequent sections.

6.2 Binocular Stereo Camera

The Videre© STOC camera outputs a point-cloud directly, alleviating the need for onboard disparity matching. The camera is tilted downward at approximate 40°, providing a maximum viewing (obstacle-detecting) distance of 4m. Using 3-point RANSAC we extract the ground-plane, and classify

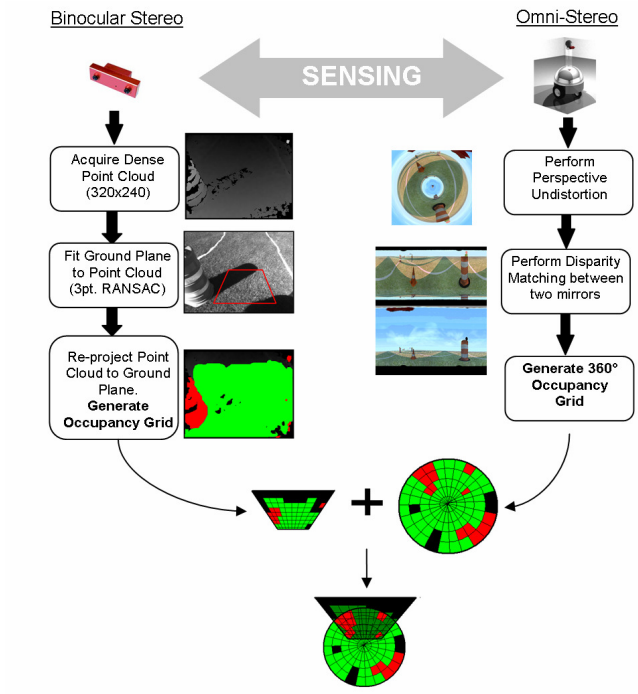

Figure 10 Fusion of two vision sensors

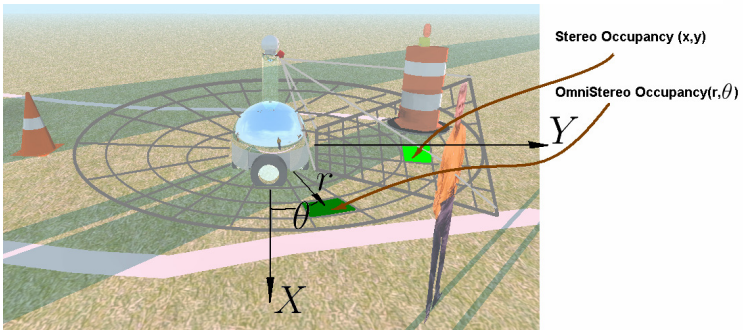

Figure 11 Rectilinear and polar occupancy grids

the pixels as *obstacles* or *free-space* based on their distance from the recovered ground plane. Using the Videre API, which provides the calibration parameters of the camera, we remap the classified

pixels into *xy* coordinates with the robot in the center, and down sample them to the occupancy grid dimensions (50x50). The probability of an occupied cell Pr(*x,y*) is given by the normalized distance of the point from the recovered ground plane.

6.3 Omnidirectional Stereo Rig

6.3.1 Color Segmentation

A process for recovering depth from the omnidirectional stereo rig is different. Instead of approaching it using a standard-technique of disparity matching (which had proved unrobust during simulations due to the limited resolution and distortion of the mirrors), we decided to match color-segmented regions. The technique is essentially based on learning the color of *free-space* (which is fairly constistent in the competition) and segmenting the *major* and *minor* images accordingly. Color-segmentation is initiated when the robot is activated. It assumes that the space immediately ahead of it is clear of obstacles (a valid assumption in the competition) and generates a Hue-Saturation Histogram of that sampled patch. From then on, the frames of the video sequence are correlated with the learned histogram to provide a measure of color-similarity. The output of the correlation is normalized to produce a probability image. Without re-learning the color of *free-space*, however, the robot would quickly get confused in shades and in patchy grass. Our approach is to mask the incoming images with the probability image (effectively masking all obstacles) and *relearn* the histogram of *free-space*, therefore providing a closed-loop control of segmentation.

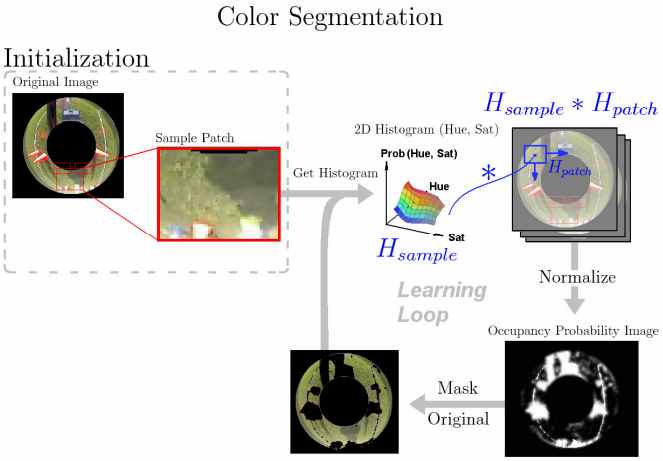

Figure 12 Omnidirectional color-segmentation flow-chart

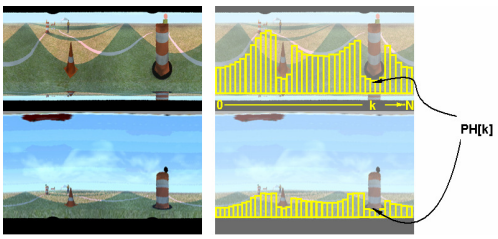

Figure 13 Area-based matching of polar histograms

6.3.1 Area matching

Both the *minor* and *major* images are segmented along the same scheme. This in effect produces a 360° histogram of free-space that can be matched between the images. If the obstacle is on the ground, then its observed location in the two images (after performing homographic transformation between the images) will be the same. This concept is similar to disparity matching, but is more robust because it exploits global information about space, rather than local point-based matching.

6.4 Distance at which objects are detected

Due to the nature of the omnidirectional mirror, it can theoretically see to the horizon (**infinitely** far). However, the limited resolution (320x240) of the image frame ensures poor depth resolution near the periphery of the mirror. Below we estimate depth-sensing accuracy of the two sensors

Sensor	Maximum Distance of Sensing	Depth Error @ 1m
Omni-stereo	Infinity (horizon)	0.34m
Videre© Binocular stereo (titled 40°)	4m	2.5cm

7 Lane Detection

The two challenges to the vision system in ELVIS (IGVC'09) were 1) false-positives from bright obstacles and 2) tight curves. CITY-ALIEN deals with these problems as follows:

- **False positives** We utilize the probability image obtained from color segmentation to mask all obstacles – essentially eliminating false positives at their root. First, the original image (*minor* image is used) is undistorted to a bird's eye view (perspective) to uncover the true geometry of painted lanes. The Occupancy Probability image (obtained from color segmentation described above) is binarized (by thresholding at 80% probability of occupancy), eroded and dilated before masking the perspective image. This ingenious heuristic allows the original image to keep thin obstacles (lanes) and only remove large obstacles (barrels, barricades, etc.). The heuristic has proven highly successful in practice.

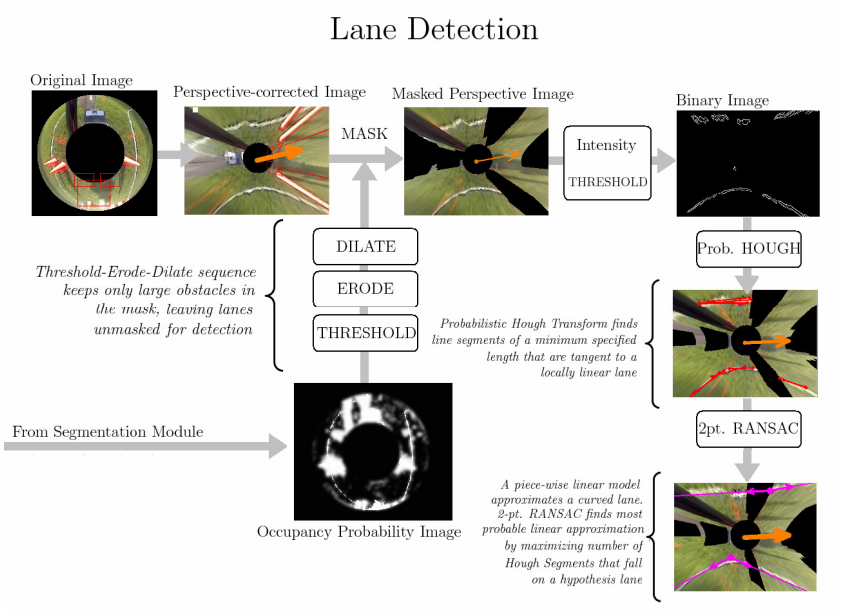

Figure 14 Lane detection flow-chart

- **Tight Curves** For the first time in 4 years of City College participating in IGVC, a non-linear model of a lane is used. Not only does a linear model fit poorly to curves, but sometimes it fits the farther end of the curve, giving the robot an early command to turn. We eliminate the problem by modeling a lane as a *piece-wise linear function*. Piece-wise linear approximation has all the simplicity of a linear model, and the robustness of more complicated parabolic or parametric curves (because the lanes don't curve too much). The masked perspective image is first binarized (thresholding Intensity in the HSI space), and then short linear segments are extracted using Probabilistic Hough Transform (the assumption of local linearity holds in curves). Two-segment RANSAC then finds the best piece-wise lane that fits through the linear segments extracted with the Hough Transform.

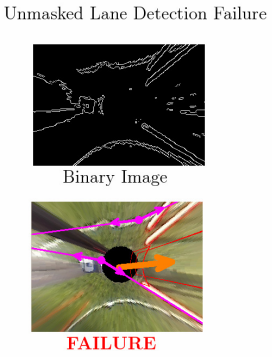

Figure 15 False-positive lane in presence of obstacle clutter

Figure 15 clearly demonstrates the affect of masking the perspective image prior to lane detection. The presence of bright cones results in false-positives. Compare to masked version in Figure 14.

7.1 Broken (dashed) Lanes

Our approach to dealing with dashed lanes is not to deal with them. RANSAC algorithm described above would be immune to short brakes (shorter than the width of the image frame) due to its global nature. Our Lane detection is used to give direction to the path planner, and

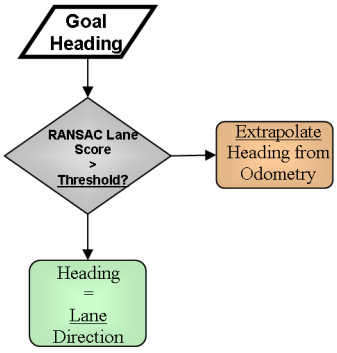

Figure 16 Lane direction estimator finite state machine (FSM)

as long as the direction is available, the robot will not travel out of bounds (even if lanes are broken). Therefore, our solution is to keep track of *lane direction* (instead of lanes) at all times, even when the lanes are not detected. For that we utilize a state-machine that switches between direction extracted from lanes (if the confidence of RANSAC is high) to extrapolating direction from odometry (when the lanes are invisible). Thus if the robot is not seeing the lanes (whether they are broken or blocked), during maneuvering, it will not loose the goal heading.

8 Obstacle Avoidance

We utilize a modified Vector Field Histogram (VFH) algorithm to drive the robot around obstacles. VFH requires a polar representation of occupancy around the vehicle, and for that purpose the occupancy grids obtained from the Binocular Stereo camera and the Omnidirectional Stereo rig are fused probabilistically (using log-odds Bayesian rule) into a common polar occupancy grid and converted into a one-dimensional 360° polar histogram (PH[k]), where k=1..N (N is the number of samples in the histogram, typically 50), and each bin of the histogram is 360°/N degrees. The combined polar histogram is thresheld at *three* distance limits (1m, 5m, 10m) with hysterisis (±1m). This provides the vehicle with *near*, *medium* and *far* ranges of sight (partially avoiding the local minima phenomena of local path planners such as VFH). The drive direction (H_{drive}) is then chosen by minimizing the following heuristic:

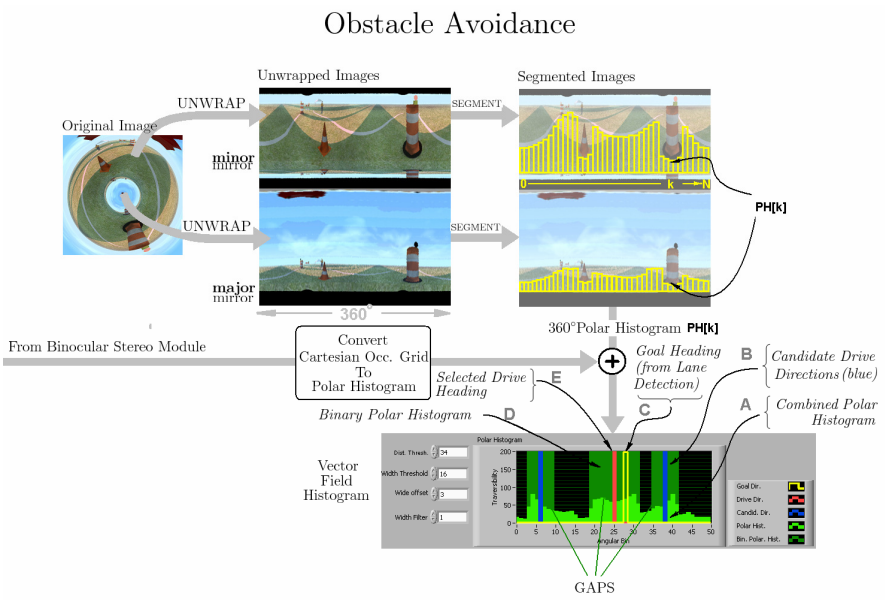

Figure 17 Vector-Field Histogram algorithm for obstacle avoidance

$$H_{drive} = \underset{H_{drive}}{\operatorname{argmin}} \left(K_g * (H_{drive} - H_{goal}) + K_p * (H_{drive} - H_{previousdrive}) + K_f * (H_{drive}) \right)$$

Where H_{drive} is the drive heading chosen by the algorithm, H_{goal} is the goal heading from lane detection, $H_{previousdrive}$ is the last chosen drive direction, K_g, K_p, K_f are weights that determine how "strong" the robot wants to 1) track the current goal, 2)stay on the current path 3)move forward. Choosing the constants equates to tuning the controller and was approached experimentally. Drive directions are prioritized from *far* to *near* range, such as to make the planner anticipate obstacles from far away

8.1 Reaction Time Reaction time of our VFH algorithm is a function of two factors – *processing speed* and the *distance at which obstacles are detected*. The VFH algorithm runs at 20Hz (50ms), and obstacles can be detected as they appear over the horizon (Section 6.3). With the *far* range look-ahead mode of the VFH, the vehicle begins to maneuver around an obstacle the moment it appears in its field-of-view. Therefore, the reaction time to an obstacle is at most 50ms.

8.2 Center Isles The heuristic in the equation above provides the means for avoiding the oscillation typically associated with obstacles in the center. It typically occurs from the indication of the VFH controller in choosing a gap if both are equally spaced (angularly). Prioritizing the current choice by making $K_p > K_g$ provides a mechanism for committing to a selected gap, and thus alleviates the oscillation.

8.3 Traps From experimentation and simulation, traps typically result in the absence of gaps in the frontal direction. But because the omnidirectional stereo system can see 360°, there is always a path, even if its behind. Although frontal directions are prioritized by K_f in the absence of frontal choice, the robot will execute a turn-on-the-dime naturally when it tries to track the gap behind it. Most importantly, it will not backtrack forever, as the original direction is estimated by odometry (Fig. 16) and once the gaps towards the correct directions become open, the robot will resume on the correct path.

8.4 Switchbacks Because of the inherent knowledge of "forward" using direction extrapolation from odometry, a switchback will not cause the robot to turn around and track back. While it might locally make a 180° turn, the memory of the "forward" direction will persist, and thus cause it to rotate back into correct direction.

8.5 Potholes The nature of color-based segmentation treats patches of different color as obstacles. Therefore, blobs of distinctly different color (such as fake or real potholes) would be avoided without adding special cases.

9 Software Architecture

Software architecture decision was based on the balance between *innovation* and *improvement* (over 2009 platform). The drivers for motion control, as well as path planning were already maintained and tested in LabVIEW, while the vision portion (for processing the Omnidirectional stereo and Binocular stereo head) was written in OpenCV in C++ from scratch. The software can be divided into three categories based on the hierarchical level:

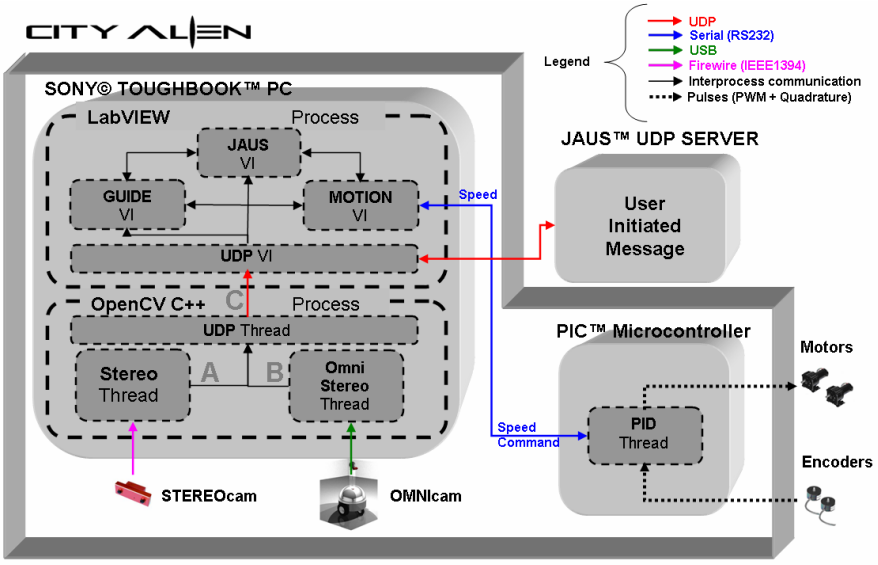

Figure 18 Software Architecture of City-ALIEN

- **LabVIEW Process** *(Highest Level)* Responsible fusing occupancy grids received from Vision (through UDP), high-level path planning (VFH), Navigation (GPS), Communication with motor controller. LabVIEW process runs on Panasonic © ToughBook™ PC
- **OpenCV C++ Process** *(Middle Level)* Responsible for processing two cameras (omnistereo + binocular stereo), detecting lanes and communicating the Occupancy Grid to LabVIEW process through UDP. OpenCV C++ process runs on Panasonic© ToughBook™ PC
- **Microcontroller** *(Low Level)* Responsible for maintaining *closed-loop* speed control based on the speed commands received from LabVIEW process (Serial) and relaying the PWM signal to the H-Bridge Motor controller. Closed-loop speed control (PID) runs on Microchip© PIC™ Microcontroller.

Between LabVIEW, OpenCV and the JAUS server, all communications are handled through UDP. Each data channel is assigned a port on a loopback address (127.0.0.1) with the exception of the JAUS server (where the port and address are specified). For example in Figure 18, the Occupancy Grid from Stereo Thread (in OpenCV process) and the Occupancy Grid from the Omni-stereo Thread (in OpenCV process) get delivered along the unique ports to LabVIEW running

concurrently, which then fuses the grids (in GUIDE VI) and directions motion commands to MOTION VI, which through a serial link, commands the microcontroller to maintain a given speed.

10. Mechanical Design

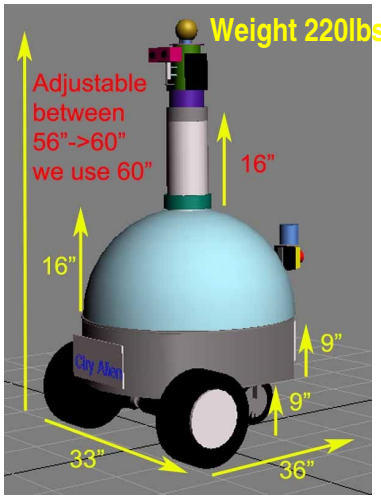

Figure 20 Dimensions

3D Studio MAX CAD software was used to develop the design drawings for manufacturing the platform. With the severe constraints on the external geometry of the system (from vision), the design had to accommodate these requirements in a unique way. The structure of the vehicle is divided into three parts, the base, the middle, and the top shelves. The base structure contains the drive train equipment, as well as the batteries, the charger and the DC-DC converter (see Section 11 for Electrical System) as shown in Figure 19A. The middle shelf structure contains most of the electronics including the laptop and its charger, the inverter, our custom made electronic box, the mechanical E-Stop, and the remote control receiver, as shown in Figure 19B. Finally, the top shelf contains mostly our innovative vision system, including the mono camera, tube, GPS, the compass, and wireless E-Stop, as shown in Figure 19C. An acrylic mirror-finish dome rests atop the top shelf (Figure 19D).

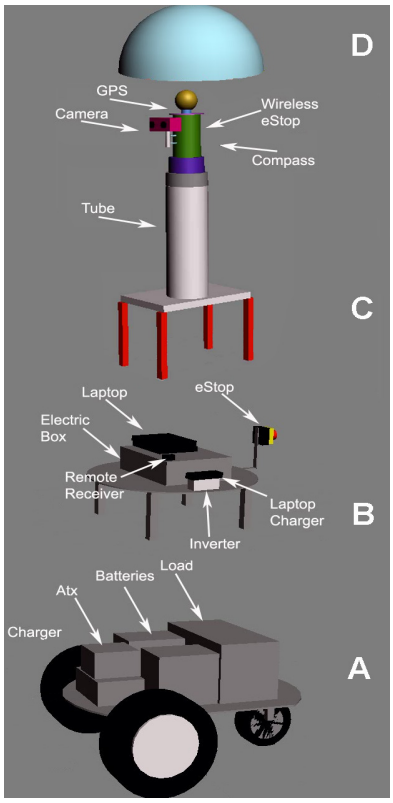

Figure 19 Exploded view

The chassis is made of aluminum T-6000 sheets, due to its weight versus strength properties. To achieve the best possible stability, we focused on putting the center of gravity as close to the ground as possible. To achieve easy troubleshooting we created a lift mechanism to our dome as shown in Figure 21. When in its down position, it has to be water proof, and in the up position, we should have access to the electronic components. The middle and top parts are designed with the largest possible space for future implementations. All the legs holding the shelves are made of aluminum squared of 1"x1" to reduce the robot's weight, in addition to the 0.125" thickness sidewalls. The dome we are using is 0.125" thick and therefore too brittle to be left unprotected. A circular acrylic plate of 16" radius was installed to add 1" safety margin around the dome.

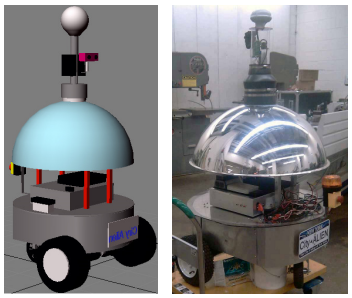

Figure 21 Lift Mechanism

10.1 Actuators/Drive System

1/8th HP Bison Permanent DC Gear Motors with a **1/10 gear reduction** ratio were used in the vehicle. The two motors were displaced near the front of the platform (where the Center of Gravity is concentrated) in a **differential drive** configuration. The radius of turn during maximal turn rate (motors rotating in opposite directions at equal speed) is 1.1m (a distance from the center of the wheelbase to the most distant point on the robot).

11 Electrical System

The electrical system was designed completely from scratch in 2009 – down to the transistor level of the H-Bridge Motor Controller. This year we incrementally improve upon last year's design. One major innovation – *Dynamic Braking* addresses the problem that we encountered in the competition – uncontrolled acceleration during descent from the ramp. The founding principles behind the organization of the electrical system are:

- **Safety**
    - **Isolated E-BOX** We approach the problem of electrical safety seriously. That was the primary reason to concentrate all of electronics inside a **single, metal monolithic** enclosure (E-BOX). The grounding of the box with the chassis provides a large grounding area (preventing ground-loops), as well as eliminates all high-power connections and electronics (H-Bridge) from the operator.
    - **Collision STALL safety** It is a dangerous situation when the robot encounters an immovable object (such as the wall), or worse – pushes a person against the wall. The inherent nature of the *closed loop* speed control will cause the motors to increase torque until they stall. If the stall condition is detected, it can then be prevented. We detect the stall by calculating the amount of current drawn by the motors plus extra current from the remaining electronics. Stall current can be found by measuring the resistance of the motor windings and using Ohm's law. In our case, the calculation yields 10A of stall current for each motor, 20A for both, plus 6A of current drawn by electronics, amounts to 26A in total. Therefore, we use a 25A circuit breaker in the system, which shuts down the robot during a stall.
    - **Waterproofing External Connections** An AC receptacle for a charger has been covered with a marine-grade waterproof AC receptacle cover. A MASTER switch has been given dual protection – a switch guard (to prevent accidental engagement), and a rubber sleeve to prevent water from seeping in through the switch.
- **Maintainability** A central hub for the electronics (E-BOX) provides an easy access to the entire system – without the need to find individual connections in different locations. In addition, the box is easily removable, and therefore can be fixed outside the vehicle. In addition, many components (such as relays) are hot-swappable – allowing the robot to be fixed without having it to be shut down.
- **Scalability** The E-BOX also allows us to adapt the electronics to any other robotic platform. In fact, this is what allowed us to redesign the entire robot, without sacrificing the investment into the electronics in 2009. Transferring the electronics is as simple as making all the external connections and flipping a switch.

11.1 Power Distribution

The system derives power from **two 40Amp-hours 12VDC Sealed Lead Acid Batteries** connected in series to provide a total voltage of **24VDC** and a total **energy capacity of 960 Watt-hours**. For convenience, the system can be operated either directly from the batteries or through an onboard **500W** charger/power supply that is connected in parallel to the batteries and is able to provide sufficient power to operate all systems (power consumption is detailed below), while simultaneously charging the 24VDC battery pack. Voltages required by the system are **12VDC** (Wireless router – for remote debugging, Inverter – for powering PC), **5VDC** (GPS, Serial Port hub, Wireless E-Stop receiver, Encoders, PNI Compass). DC-DC conversion is performed by a dedicated **500W ATX DC-DC converter**, and a standard vehicle **inverter** provides onboard 120VAC for powering the computer.

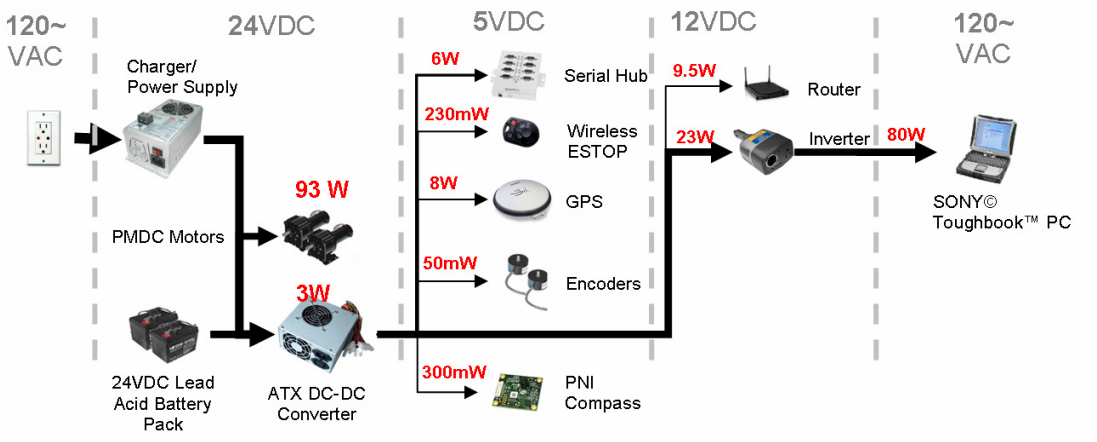

Figure 22 Power distribution and consumption chart

11.2 Power Consumption

Estimated charge time (with system off), from experimentation, is **5 hours**. We carry an extra battery pack in the competition that will provide us with the ability to test practically without interruption for recharging. Compare the charge time to the approximate operating time of the vehicle with all systems on (all electronics+PC), and in motion (5.8 hrs – obviously the figure depends heavily on how "hard" the robot is driven (speed and inclines). The figure is based on a long-term running average from our continual testing below 5mph on relatively flat terrain). While the robot is operating with fresh battery back, the old one can be recharged completely.

System State	Power (W)	Operating Time (full charge)
All Systems ON + Driving (avg)	170	~5.8hrs
All Systems ON + Stationary	130	~7.6hrs
IDLE (only DC-DC converter on)	3	~2 weeks

The idle state figures are of theoretical interest, because 3W is the amount of power consumed by the DC-DC converter to provide all the necessary voltages (5VDC, 12VDC) to run the remaining systems. This power is essentially "wasted" in the conversion process.

11.3 E-BOX: Internal Power Distribution

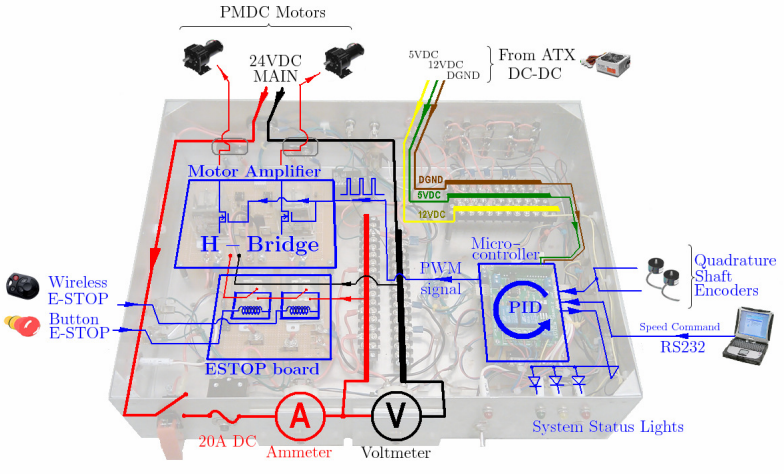

Figure 23 E-BOX layout

The purpose of the E-BOX is to interface high-level logic (PC) with the hardware (motors), while providing essential low-level control (switches, circuit-breakers) and measurement (volt, amp-meter) interface over the entire electrical system. Every electrical component of the E-BOX was built at chip-level with maximum customization to fit our budget and performance requirements. The components of the E-BOX and their functions are summarized:

- **PIC Microcontroller** Tasks: signal processing, communication the PIC microcontroller board interfaces directly to the PC through the serial port link (RS-232) over which a custom-formatted ASCII protocol commands the wheels to rotate with a given RPM ("M1###M2###"; where ### is the desired RPM of the respective motor). The custom PID routine in the PIC executed every 20ms counts the number of pulses from a quadrature encoder on each wheel (within 20ms) which is then converted to the actual RPM (in our case *512 encoder pulses/wheel revolution*). The difference is then fed into the PID controller (Fig.20), whose parameters were tuned online with the heuristic Ziegler-Nichols to achieve a desired response time and minimal overshoot. The output of the PIC is a **Pulse-Width Modulated** wave (whose width is directly proportional to the torque of the motors) with a frequency of 1KHz (reason given below). The PWM wave (along with direction bits CW/CCW) is fed to the H-Bridge.

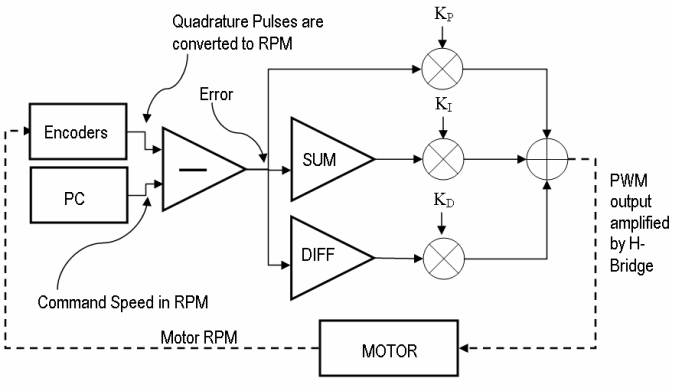

Figure 24 Internal PID *closed-loop* speed control

- **H-Bridge** Tasks: Driving motors The custom-designed H-Bridge board (details in the next sub-section) converts the 5Vpp PWM signal into 24Vpp PWM that is capable of sourcing and sinking up to 70A of DC current (using High-power MOSFETS). The output of the H-Bridge feeds the motors directly.
- **E-Stop Board** Tasks: Interrupting power to H-Bridge The supply voltage to the H-Bridge can be interrupted with two relays connected in **series** – a **button** and **wireless** E-STOP relays (Fig. 30 in section 14). As a result, when one E-STOP is triggered, the power to the motors is cut-off without cutting off the power to the entire system.

11.4 Electrical Innovations

11.4.1 Dynamic Braking with H-Bridge

As outlined earlier, braking is an essential feature when the vehicle is heavy (ALIEN weighs 220Lbs). All permanent magnet DC motors can be stopped when their contacts are shorted. While shorting the motor leads can be done with a simple relay, it does not give the continuity of control of braking that is desired. We solved the problem by introducing MOSFETS that essentially disconnect the motor from the H-BRIDGE and short the leads. The advantage is that the MOSFETS may be pulsed by the PIC microcontroller at high frequency with a PWM wave, creating an effect of a continually variable brake-power. Figure 24 illustrates the "before" and "after" of the modified H-Bridge. The 2009 H-Bridge is a single "drive" MOSFET and two relays that act to reverse the polarity of the motor. The modified H-Bridge (Figure 25B) introduces three MOSFETS (T2, T3, T4). When T2 and T4 gates are brought low, and T3 pulsed with a PWM wave, the motor is in the "brake" mode. The

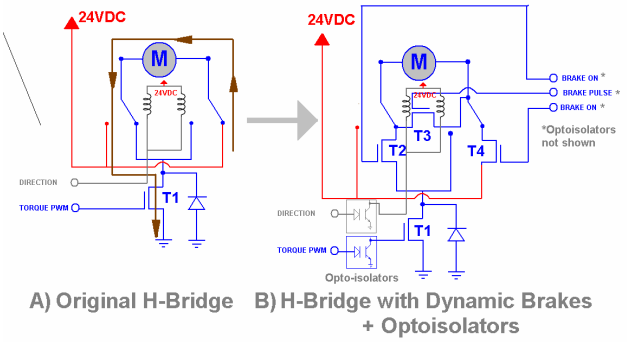

Figure 25 "Before" and "After" in the H-Bridge design

innovation proved successful, and the robot is able to produce moderate brake power when moving at speeds > 1MPH. This strength of the brake is directly proportional to the speed at which the vehicle is moving.

11.4.2 Optical Isolation of Logic and Power

One common problem with mobile robots is the lack of true ground. This creates the so-called "ground loops" when the grounds of different parts of the system are not on the same voltage. The problem often appeared in our vehicle as noise in the communication system, and last year was partially alleviated by robust communication algorithms (parity and checksums). This year we isolated motor power (24VDC bus) from the logic power (5VDC, 12VDC) inside the H-Bridge by introducing optical-isolators (Fig. 25B). The problems with noise in communication lines had disappeared.

12 Navigation Challenge Strategy

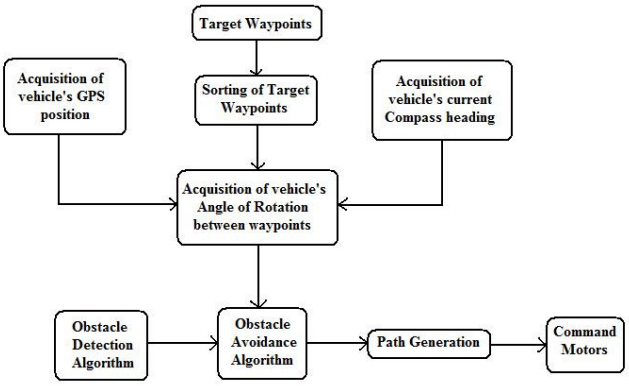

Figure 26 Navigation challenge flowchart

The Navigation Challenge algorithm uses reliable data from the NovAtel smart antenna (Easting std. < 0.4m, Westing std. <0.75m) with OmniSTAR VBS corrections, the PNI TCM5 3-axis digital compass and the Initial Waypoints to find an Angle of Rotation between waypoints with respect to true north. Initial Waypoints are sorted out to find the shortest overall path by implementing a Dijkstra's Algorithm. A block diagram overview of this algorithm is shown in Figure 26. Once the angle of rotation is obtained, it will be transferred to our obstacle avoidance algorithm (VFH) which will generate a new navigation path and command the motors to follow it. When City ALIEN reaches the last target waypoint, it will return to the initial starting position and cease motion indicating that the mission has been accomplished.

12.1 Testing

We tested the Navigation Challenge Algorithm by simulating it in LabVIEW. We then proceeded to test it on an open area by making our own waypoints around The City College of New York's campus (Figure 27) After selecting a set of target waypoints, as seen in Figure 27(left), our sorting algorithm determined the shortest path, denoted by the black lines in Figure 27(right), by using the **Dijsktra's Algorithm**. The selected path was then traversed by the robot, and the statistical log of arrival accuracy was generated to estimate the accuracy of the navigation system:

Figure 27 City College of New York waypoint test setup

Error Heading	Std. Deviation (σ)	Number of trials (N)
Northing	0.75m	34
Easting	0.4m	34

As expected North-South standard deviation is larger than the East-West deviation, but both satisfy the accuracy requirement of the competition.

12.2 Competition Data

We tested the performance of the sorting algorithm on the previous waypoint data from the IGVC competition (Figure 27). It can be shown that the total distance traveled is the shortest possible. Of course, we understand that in the presence of obstacles the importance of sorting is reduced, however we assume that the distribution of obstacles is fairly sparse (from past observations) and thus would make sorting important.

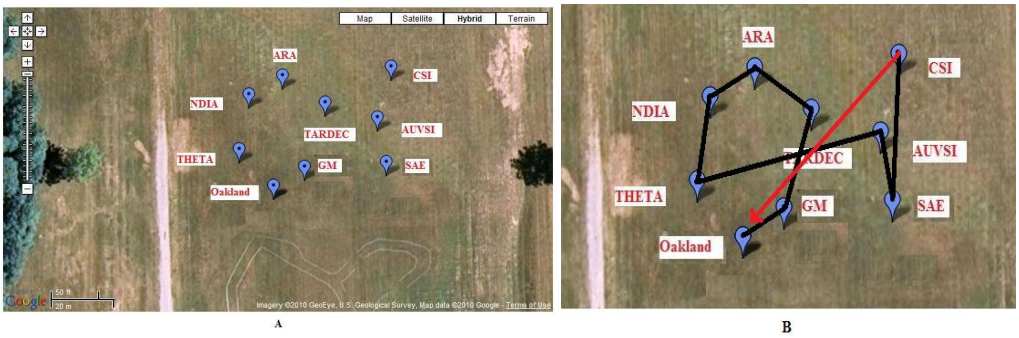

Figure 28 Oakland University waypoints

13 JAUS strategy

This year is the first time that the City College of New York is participating in the JAUS challenge. Because the software architecture of the vehicle is inherently UDP-based, adding a JAUS server can be abstracted as adding another process within the architecture. For this reason, LabVIEW receives and sends JAUS messages from the same thread as the internal messages (such as those to and from OpenCV C++ Vision Process), however an additional software layer processes the messages and responds to them by sending higher-level control commands to the navigation and motion software.

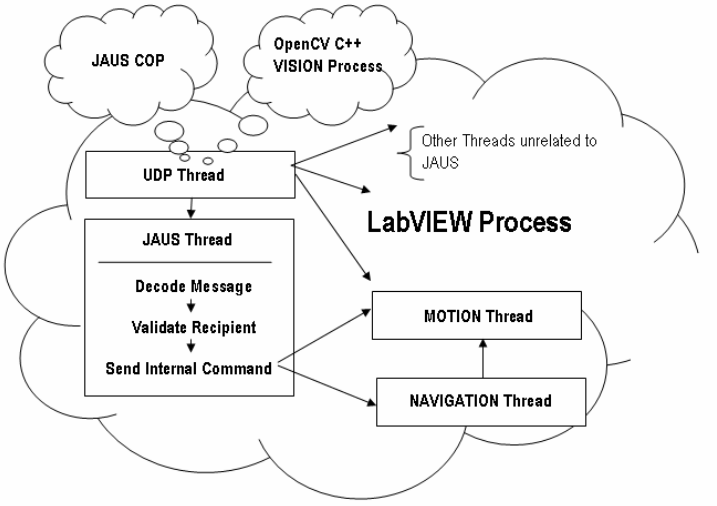

Figure 29 JAUS Implementation within City ALIEN's software architecture

14 E-STOPs

Wireless and Button E-STOP on the E-STOP board in the E-BOX and are connected in series to disconnect power from the H-Bridge when at least one has

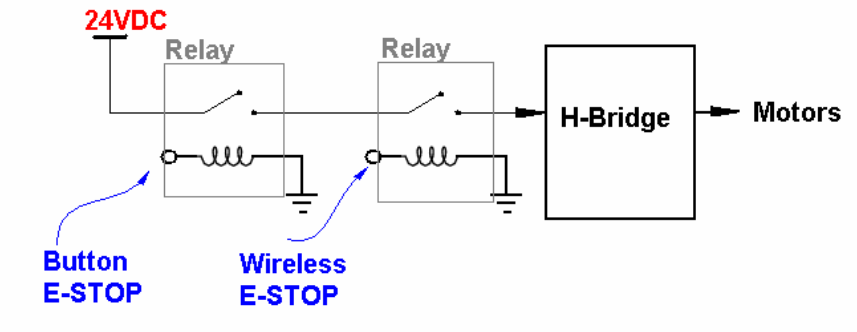

Figure 30 E-Stop wiring

been triggered. The wireless E-Stop has been executed with a standard garage-opener key-fob and a rolling code 310MHz AM receiver with a range over 250 feet. The Wireless receiver module is mounted at the top of the mast as to maximize line-of-sight exposure and minimize electromagnetic interference from the motors.

15 Physical Performance Characteristics

Physical performance characteristics of the vehicle were estimated at design time to ensure satisfying competition requirements. First – a rough weight estimate of the robot was made, based on the past year's vehicles (since the electronics were mostly the same) and the volume ratio (since the material was the same, the volume ratio gave a good estimate). The estimated weight prior to design was to be between 150-250lbs, and the actual weight after construction is 220 lbs. Knowing the weight, RPM of the motors (170rev/min), torque(40ft-lbs), wheel diameter (10"), we were able to predict the performance and compare to the data from our tests:

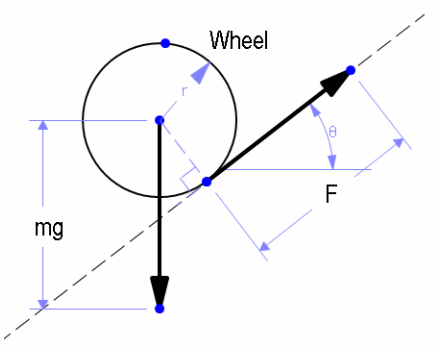

Figure 31 Calculating maximum incline slope

- **Calculating maximum speed** We calculate the maximum speed based on the RPM and the circumference of the wheel: $2\pi r * RPM$.
- **Calculating maximum ramp slope** Maximum angle of incline is when $Mg\sin\theta = Tr$, where T is motor torque, M – mass of robot, r – the radius of the wheel, and θ the angle of the incline. We solve for angle to determine the maximum incline slope.
- **Calculating minimum turning radius** Minimum turning radius (when motors are rotating in opposite directions with equal speed) depends on the largest offset of the wheels from the edge of the body = 1.1m.

Performance	Predicted	Actual
Maximum Speed	5.05mph	4.8mph
Maximum ramp slope	23°	19°
Minimum Turning radius	1.1m	1.1m

16 Cost breakdown

The cost this year has been significantly reduced to the increased support and awareness from various departments in the university. In the cost-breakdown, the items which we count in the "cost to team" column are those which have been purchased directly out of allotted funds for the competition. These funds came from the IGVC Club (which was organized to raise funding), the Dean and Departmental (Elec. Engineering) funding. Mentor Dr. Xiao purchased equipment on his own grant money, which we do not include in the "cost to team" column.

Item	Cost	Cost to Team	Fund. Source
Videre© Stereo Camera	$1,200	$0	Robotics Lab
Logitech Pro-9000 Camera	$69	$69	Club Fund
Large Mirror dome	$180	$180	Dept. Fund
Cast Acryllic Tube (transp)	$250	$250	Dept. Fund

Novatel GPS Receiver	$1,300	$0	Robotics Lab
TCM PNI Compass	$1,000	$800 (acad. disc)	Dean Fund
SONY© Tougbook™ PC	$5,600	$0	Robotics Lab
Wireless E-Stop receiver	$80	$80	Club Fund
Construction materials (metal)	$1,900	$0	Mech. Eng. shop
Construction materials (tools)	$1,600	$0	Mech. Eng. shop
Misc. Electronic parts	$450	~$200	Electronics Lab
Total	**$13,629**	**$1,579**	

17 Man-hour breakdown

Man-hours are hard to estimate when they are not kept track of on daily basis. We estimate the hours by calculating the average number of hours worked per week and multiplying by the period of involvement.

Name	Major	Degree (graduation)	Concentration	Hours
Igor Labutov*	Comp. Eng.	Undergrad (2010)	Vision/Path planning	**520**
Erez Gati	Comp. Eng.	Undergrad(2010)	Mechanics	**600**
Carlos Jaramillo	Comp. Eng.	Graduate(2012)	Vision	**300**
Ricardo Chincha	Electrical Eng.	Graduate(2011)	Navigation	**200**
Fernando Guevara	Electrical Eng.	Undergrad(2011)	Challenge Electronics	**150**
			Total:	**1770**

Man-hours = 5*1770 = 8,850 man-hrs

18 Conclusion

City ALIEN is a truly innovative platform that has been developed with the goal of applying cutting-edge vision research (to ensure passive sensing) to practical robotics. With our unique catadioptric design, we have demonstrated that the vision-only system is capable of performing at least as well as classical designs with bulky laser range scanners. In addition, the balance between *innovation* and *improvement* that our team was able to achieve, our electronics have seen a dramatic enhancement – making City ALIEN safer, most robust and more maneuverable than any past generation of City College IGVC robots. It is no doubt that City ALIEN will demonstrate top-notch performance in the 2010 IGVC